Detection of Hyperexcitability by Functional Magnetic Resonance Imaging after Experimental Traumatic Brain Injury

Joanna K Huttunen[1]; Antti M Airaksinen[1]; Carmen Barba[2], Gabriella Colicchio[3], Juha-Pekka Niskanen[1,4,] Artem Shatillo[1]; Alejandra Sierra Lopez[1]; Xavier Ekolle Ndode-Ekane[1]; Asla Pitkänen[1]; Olli H Gröhn[1]

[1]A. I. Virtanen Institute for Molecular Sciences and [4]Department of Applied Physics, University of Eastern Finland, Kuopio, Finland.
[2]Neuroscience Department, Children's Hospital Anna Meyer, Florence, Italy.
[3]Neurosurgery Department, Catholic University, Rome, Italy.

J.K.H. and A.M.A. contributed equally as first co-authors.
A.P. and O.H.G. contributed equally as senior co-authors.

Corresponding author: Prof. Olli Gröhn A. I. Virtanen Institute for Molecular Sciences, University of Eastern Finland, P. O. Box 1627, FI-70211 Kuopio, Finland. E-mail: olli.grohn@uef.fi, phone +358-50-3590963

Key words: epileptogenesis; functional imaging; lateral fluid-percussion injury; post-traumatic epilepsy

Abstract

Diagnosis of ongoing epileptogenesis and associated hyperexcitability after brain injury is a major challenge. As increased neuronal activity in the brain triggers a blood oxygenation level-dependent (BOLD) response in functional magnetic resonance imaging (fMRI), we hypothesized that fMRI could be used to identify the brain area(s) with hyperexcitability during post-injury epileptogenesis. We applied fMRI to detect the onset and spread of BOLD activation after pentylenetetrazol (PTZ)-induced seizures (PTZ, 30 mg/kg, i.p.) in 16 adult male rats at 2 months after lateral fluid-percussion (FPI)-induced traumatic brain injury (TBI). In sham-operated controls, the onset of the PTZ-induced BOLD response was bilateral and first appeared in the cortex. After TBI, 5 of 9 (56%) rats exhibited ipsilateral perilesional cortical BOLD activation, followed by activation of the contralateral cortex. In 4 of 9 (44%) rats, the onset of the BOLD response was bilateral. Interestingly, the latency from the PTZ injection to the onset of the BOLD response increased in the following order: sham-operated controls (ipsilateral 132 ±57 s, contralateral 132 ±57 s; $p>0.05$) < TBI with bilateral BOLD onset (ipsilateral 176 ± 54 s, contralateral 178 ± 52 s; $p>0.05$) < TBI with ipsilateral BOLD onset (ipsilateral 406 ± 178 s, contralateral 509 ± 140 s; $p<0.05$). Cortical lesion area did not differ between rats with ipsilateral vs. bilateral BOLD onset ($p>0.05$). In the group of rats with ipsilateral onset of PTZ-induced BOLD activation, none of the rats showed a robust bilateral thalamic BOLD response, only 1 of 5 rats had robust ipsilateral thalamic calcifications, and 4 of 5 rats had perilesional astrocytosis. These findings suggest the evolution of the epileptogenic zone in the perilesional cortex after TBI, which is sensitive to PTZ-induced hyperexcitability. Further studies are warranted to explore the evolution of thalamo-cortical pathology as a driver of epileptogenesis after lateral FPI.

Introduction

According to the World Health Organization, nearly 50 million people throughout the world have epilepsy at any one time (http:// www.who.int/mediacentre/factsheets/fs999/en/). Traumatic brain injury (TBI) is estimated to cause 10% to 20% of structural epilepsies and 5% of all epilepsies[1,2]. The risk of epileptogenesis increases according to the severity of the TBI – approximately 4-fold after mild TBI, 8-fold after moderate TBI, and 16-fold after severe TBI[3,4]. Up to 53% of patients with penetrating TBI develop epilepsy[5,6]. Seizures after TBI are often drug-refractory, and the need for medical care continues for years after a diagnosis of posttraumatic epilepsy (PTE)[1,7]. Moreover, drug-refractoriness may be associated with a multifocal seizure onset zone, which can exclude PTE patients from epilepsy surgery. Further, PTE is associated with an increased risk of death at a younger age[8]. Therefore, identification of the mechanisms of post-traumatic epileptogenesis (PTEgenesis) as potential therapeutic targets represents a major unmet medical need.

To identify the epileptogenic molecular mechanisms leading to PTE, it is important to first determine the brain areas that become hyperexcitable after TBI and then the seizure onset zone(s). Analyses of epileptogenic molecular mechanisms rely mainly on animal models, however, as human brain tissue is not usually available. TBI induced by lateral fluid-percussion injury (FPI) in adult rats results in the development of epilepsy in up to 50% of animals over a period of 1 y[9-12], consistent with the rate of development in humans with TBI[8]. The FPI-induced TBI model provides a useful tool to assess the evolution of epileptogenic tissue pathology in the injured brain. The site of seizure onset after lateral FPI has not been fully characterized.

Ex vivo electrophysiologic studies using hippocampal slice preparations from rats with lateral FPI show increased hippocampal excitability within hours post-TBI (for review, see[13]). More recent *in vivo* recordings revealed perilesional seizure onset with hippocampal involvement[9,14,15]. Although these studies indicate perilesional and hippocampal excitability, the location of the seizure onset has remained somewhat uncertain due to the limited number of electrodes in different brain areas used to assess seizure initiation.

Functional magnetic resonance imaging (fMRI) can detect blood oxygenation level-dependent (BOLD) changes in the seizure onset zone in humans[16-18]. Despite the

methodologic challenges related to fMRI studies in rodents, such as the need for sedation, small brain size, and magnetic susceptibility problems in a high magnetic field, BOLD activation in Wag/Rij rats with spontaneous absence seizures has been successfully detected with fMRI[19]. Previous studies also revealed the potential of fMRI for the detection of network activation during and after chemically induced seizures in normal rats, such as those induced by pentylenetetrazol (PTZ), which triggers a bilateral cortical BOLD increase that matches the timing and evolution of electrophysiologic epileptiform activity, expression of c-Fos, and distribution of metabolic activity[20-24]. To date, fMRI has not been used to investigate the hyperexcitability developing after epileptogenic brain injury.

The present study evaluated our hypothesis that at 2 months after lateral FPI when a subpopulation of rats undergoes epileptogenesis, the onset and spread of PTZ-induced seizures is altered due to focal network modifications induced by TBI. In particular, we expected that PTZ-induced BOLD activation would be lateralized to the perilesional cortex rather than being symmetric like that observed in control animals.

Materials and Methods

Animals

Adult male Sprague-Dawley rats (n=19, weight at the time of TBI, 362 ± 11 g) were used. Animals were housed in individual cages in a controlled environment (constant temperature 22 ± 1 °C, humidity 50–60%, lights on 07:00–19:00 h) with free access to food and water. All animal procedures were performed in accordance with the guidelines set by the Committee for the Welfare of Laboratory Animals of the University of Eastern Finland and the State Provincial Office of Southern Finland, and conducted in accordance with the European Community Council Directives 2010/63/EU.

Rats were randomized into sham-operated experimental control (n=8) and TBI (n=11) groups. Acute mortality (<48 h) was 18% in the TBI group (2/11) and 13% in the sham-operated experimental controls (1/8). The surviving 16 rats underwent simultaneous local field potential (LFP)-fMRI measurement. In two sham-operated controls, the LFP recording failed due to technical difficulties.

Induction of lateral fluid-percussion brain injury

TBI was induced by lateral fluid-percussion injury (FPI), as described previously[25,26], in 11 rats. Briefly, rats were anesthetized by intraperitoneal injection of a mixture of sodium pentobarbital (58 mg/kg), chloral hydrate (60 mg/kg), magnesium sulfate (127.2 mg/kg), propylene glycol (42.8%), and absolute ethanol (11.6%), (6 ml/kg). Craniectomy (∅ 5 mm) was performed with a trephine between bregma and lambda on the left convexity (craniotomy center: 4.5 mm posterior to the bregma, mediolateral 2.5 mm from the midline), leaving the dura intact. The injury was induced with a brief (21-23 ms) pressure fluid pulse impact against the exposed dura using an FPI device (AmScien Instruments, Richmond, VA, USA). The pressure of the impact was 3.50 ± 0.04 atm, aimed at inducing a severe TBI. Sham-operated experimental controls underwent identical anesthetic and surgical operations, but were not exposed to lateral FPI.

Electrode implantation and monitoring of provoked seizures

At 2 months after TBI or sham-operation, rats (n=16, 439 ± 27 g at the time of fMRI) were anesthetized with isoflurane (induction 5% and 1.5%-2% maintenance during surgery). To monitor blood gases and pH during the experiment, the femoral artery was cannulated using PE-10 tubing. An intravenous tube was inserted into the right femoral vein for administration of sedatives and muscle relaxants.

To record PTZ-induced epileptiform electrographic activity, a tungsten wire electrode (50-µm diameter, California Fine Wire, Grover Beach, CA, USA) was inserted into the right (contralateral) frontal cortex (3.2 ± 0.7 mm anterior from bregma, 2.1 ± 0.2 mm lateral from the midline, 0.9 ± 0.4 mm ventral from the pial surface[27]). Chloridized silver wire reference and ground electrodes were placed subcutaneously in the neck.

After electrode implantation, rats were tracheotomized (with a 13G tube) and transferred to a non-magnetic stereotaxic frame. Rats were secured in the animal holder with earplugs and a bite bar. The tracheal tube was connected to a mechanical ventilator (Harvard Apparatus), and the animals were ventilated with a mixture of 70% N_2 and 30% O_2. Breathing rate was set between 60-65 breaths/min, and breathing volume was approximately 2.7-3.1 ml per breath depending on the weight of the rat. Arterial blood samples for blood gas analysis were obtained before (baseline) and at the end of the fMRI measurements.

To prevent motion artifacts during fMRI, rats were sedated with a bolus of medetomidine (0.05 mg/kg, i.v., Orion Pharma, Espoo, Finland) and paralyzed with pancuronium bromide (1 mg/kg, i.v., Organon, Oss, Netherlands). Ten minutes after bolus injection, sedation and paralysis were maintained with a continuous intravenous infusion of a mixture of medetomidine (0.1 mg/kg/h) and pancuronium bromide (2 mg/kg/h). Five minutes later, the isoflurane was discontinued.

Simultaneous recording of field potentials and BOLD fMRI

Simultaneous LFP and fMRI measurements were started approximately 45 min after switching the anesthesia from isoflurane to medetomidine sedation. During this period, the medetomidine sedation reached a steady state, and the effects of isoflurane on brain activity became insignificant.

MRI measurements were performed with a 9.4 T horizontal scanner interfaced using a Varian DirectDrive^{TM} console (Varian Inc., Palo Alto, CA, USA). For signal transmission and reception in fMRI experiments, an actively decoupled volume radiofrequency coil and 4-channel array receiving coil were used (RAPID Biomedical GmbH, Rimpar, Germany). A fast-spin echo multi slice (FSEMS) sequence was used to collect anatomic images [TR 5.4 s, effective TE 48 ms, echo spacing 16 ms, 8 echoes/excitation, field of view of 5.0 x 5.0 cm^2, image matrix of 512 x 512, resolution 98 x 98 μm^2, slice thickness 0.75 mm, 40 slices].

The fMRI data were collected using a single-shot spin-echo echo-planar-imaging sequence (TR 4 s, TE 40 ms, field of view of 2.5 x 2.5 cm^2, image matrix 64 x 64, resolution 391 x 391 μm^2, slice thickness 1.5 mm, number of slices 15). The fMRI data from 15 slices were collected during the first second of the TR, leaving a 3-s uncontaminated LFP electrophysiologic signal between the MRI artifacts. The LFPs were monitored from the contralateral cortical electrode during the entire fMRI measurement using a BrainAmp MR plus magnet compatible system (Brain Products GmbH, Munich, Germany). The electrographic signal was low-pass filtered at 1000 Hz (sampling rate 5000 Hz).

Image acquisition started with 1000 images captured as a baseline. Seizures were then induced by intraperitoneal injection of PTZ (30 mg/kg; 1,5-pentamethylenetetrazol, 98%; Sigma-Aldrich YA-Kemia Oy, Finland) dissolved in sterile 0.9% saline (4 mg/ml solution). Each

rat received a single injection of PTZ[28]. Image acquisition was continued for 1000 images, resulting in a total of 2000 images per rat.

Histology

After completing the electrophysiologic and fMRI recordings, rats were deeply anesthetized with isoflurane and decapitated. Brains were removed from the skull, immersion-fixed in 4% buffered paraformaldehyde for 4 h, and cryoprotected in a solution containing 20 % glycerol in 0.02 M potassium phosphate buffered saline, pH 7.4, for 24 h. The brains were blocked, frozen in dry ice, and stored at 70 °C until cut. The brains were sectioned in the coronal plane (30 μm, 1-in-5 series) using a sliding microtome. The sections were stored in a cryoprotectant tissue-collecting solution (30% ethylene glycol, 25% glycerol in 0.05 M sodium phosphate buffer) at 20 °C until processed.

Adjacent series of 1-in-5 sections were stained for thionin to assess lesion location and extent, myelin [0.2% gold chloride method;[29]], astrogliosis [glial fibrillary acid protein (GFAP) immunohistochemistry;[30]], microgliosis [OX-42 immunohistochemistry;[30]], iron deposits [Prussian blue;[31]], and calcifications [Alizarin red;[32]].

The extent of cortical lesion and the location of BOLD onset were reconstructed from coronal MRI slices as previously described[33]. The extent of perilesional astrocytosis was quantified by placing a counting grid on top of the section under a light microscope, and by counting the number of 100 μm x 100 μm squares with immuno-stained activated astrocytes along the edges of the lesion cavity throughout its rostrocaudal extent. Density of myelinated fibers in the S1 cortex was quantified ipsilaterally and contralaterally using ImageJ software (version 1.41o, http://rsb.info.nih.gov/ij) according to Niskanen and colleagues[34]. Calcifications in the ipsilateral thalamus (no calcifications were found contralaterally) were scored from 1-3 based on their size and maturity as described by Lehto and colleagues [35]. Representative examples of calcium deposits and corresponding scores are shown in **Supplementary Fig. 2**.

Analysis of fMRI data to determine the onset region of the provoked seizures

The fMRI data were converted from native imaging software formats to NifTI using Aedes (http://aedes.uef.fi). The fMRI data were preprocessed including motion correction, co-registration, and spatial smoothing using SPM8 (Wellcome Department of Imaging Neuroscience, UCL, London, UK) and Matlab (Version 2012b, The MathWorks Inc., Natick, MA, USA). Slice-timing correction was not performed as the acquisition time for all slices in a volume was < 1 s. A reference brain template was created from one sham-operated animal, and all fMRI data were co-registered to it for group level visualization. Spatial smoothing was performed using a 2 x 2 pixel full-width at half-maximum Gaussian kernel. A Gaussian hemodynamic response function (HRF) was used instead of the default canonical HRF used in SPM8. The parameters of the Gaussian HRF were selected to reflect the temporal characteristics of the measured rodent HRF reported by Silva and colleagues[36], resulting in an HRF peaking at 2 s and returning to baseline at 5 s.

To assess the location of the provoked seizure onset, a short boxcar block analysis was performed. Due to the long baseline period, 150 baseline images captured before PTZ administration were used for the analysis. A sliding window of three images was used for the activation period. The timing was based on visual inspection of the BOLD time series. Statistical analysis of those 153 images was performed using the general linear model on a voxel-by-voxel basis[37]. Activated brain areas were assessed using a one-sample t-test thresholded at $p < 0.05$ (false discovery rate (FDR) -corrected). To detect the center of the activated region, a weighted average was calculated from the thresholded T-map for all activated regions with a region size > 4 pixels in plane. The location(s) of the BOLD response(s) evoked by the PTZ-induced seizure was then normalized to the anatomic images of the reference brain.

The voxel-vise onset times were visualized by shifting a 3-volume-long positive boxcar block over a time-series of 400 s after the onset of PTZ activation with 20 s interval (Fig. 3). Every block was tested separately from the others. In order to correct for multiple comparisons, we performed FDR-correction for all p-values from all the tests and all the animals.

Statistical analysis

Statistical analysis was performed using SPSS for Windows (*v.* 23) and Excel. Comparisons between animal groups were made with the non-parametric Kruskal-Wallis test followed by a *post hoc* analysis with the Mann-Whitney *U* test. Interhemispheric differences were analyzed using Wilcoxon's test. Difference in astrogliosis along the rostrocaudal extent of lesion between the animals with ipsilateral and bilateral BOLD onset was analysed using repeated measures ANOVA, followed by *post hoc* analysis with Dunnett's test. Correlations were calculated using Spearman's rho test. A p value <0.05 was considered significant. All data are presented with mean ± standard deviation (SD) or standard error of the mean (SE) as indicated in the text.

Results

Acute mortality, apnea time, and occurrence of post-impact seizures

Rats with TBI were divided into two subgroups based on whether the onset of the PTZ-induced BOLD response was bilateral or ipsilateral **(Figs. 1-3)**. In the whole group, the mean duration of post-impact apnea was 31 ± 10 s. Time in apnea did not differ between rats with bilateral (29 ± 3 s, n=4) and ipsilateral (33 ± 13 s, n=5) onset of PTZ-induced BOLD activation. Of 9 rats included in the final analysis, 5 had acute post-impact seizures lasting an average of 36 ± 11 s. The occurrence or duration of post-impact seizures did not differ between subgroups.

Physiologic parameters during fMRI monitoring

The physiologic data are summarized in **Table 1**. All physiologic parameters were within the normal range in all animals during the experiment. In the TBI group, pCO_2 and pH were higher, and O_2 saturation lower at the end of the fMRI compared with that at baseline ($p<0.05$). Also, pH at the end of the fMRI session was lower in the TBI group than in sham-operated rats ($p<0.05$). The physiologic parameters also did not differ between rats with an ipsilateral or bilateral onset of PTZ-induced BOLD response (data not shown).

Table 1. Physiological parameters during simultaneous electrophysiologic and fMRI recordings.

Sham-operated (n = 7)	Baseline	End of fMRI
pCO_2 (mmHg)	30.5 ± 6.0	37.0 ± 4.2
pO_2 (mmHg)	117.0 ± 21.3	120.9 ± 38.6
pH	7.49 ± 0.06	7.42 ± 0.03
O_2 saturation (%)	98.5 ± 0.8	98.0 ± 2.4

TBI (n = 9)	Baseline	End of fMRI
pCO_2 (mmHg)	33.1 ± 6.0	39.1 ± 8.8 †
pO_2 (mmHg)	108.1 ± 8.1	104.9 ± 15.7 †
pH	7.47 ± 0.04	7.38 ± 0.04 *†
O_2 saturation (%)	98.7 ± 0.5	97.4 ± 1.2

Values are shown as mean ± SD, standard deviation. Statistical significances: * p<0.05 (sham *vs.* TBI group, Mann-Whitney *U*); †p<0.05 (baseline *vs.* fMRI sample in the same rat, Wilcoxon).

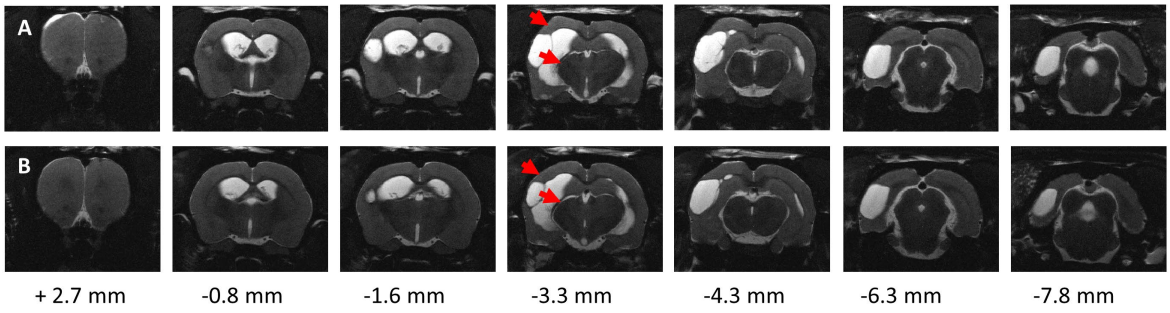

Figure 1. Anatomic T2-weighted images of two representative cases demonstrating variability in the extent of brain damage at 2 months after lateral fluid-percussion–induced traumatic brain injury. Note the atrophy in the ipsilateral cortex and thalamus (red arrows). Anteroposterior level is shown relative to bregma. **(A)** A rat with a large cortical cavity, showing rapid bilateral blood oxygenation level-dependent (BOLD) activation after PTZ administration (see **Fig. 3B**). **(B)** A rat with a smaller lesion cavity rostrally. After a PTZ administration, the animal showed longer-lasting ipsilateral BOLD activation before spreading to the contralateral side (**Fig. 3A**).

Characteristics of the BOLD response after PTZ administration in fMRI

Onset of PTZ-induced BOLD response. In sham-operated experimental controls, the onset of the PTZ-induced BOLD response was bilateral cortical. In one control rat, the onset of the bilateral cortical BOLD response coincided with thalamic activation ipsilateral to the craniotomy **(Fig. 2A)**.

In TBI animals with bilateral onset of the BOLD response, the BOLD onset occurred bilaterally in the somatosensory cortex and extended throughout multiple functional slices. In 3 of 4 bilaterally responding rats, also the thalamus became activated bilaterally. In TBI rats with ipsilateral onset of the BOLD response, the BOLD onset was located in the perilesional cortex, typically rostral to the lesion core. Thalamic involvement was delayed or not present **(Fig. 3)**.

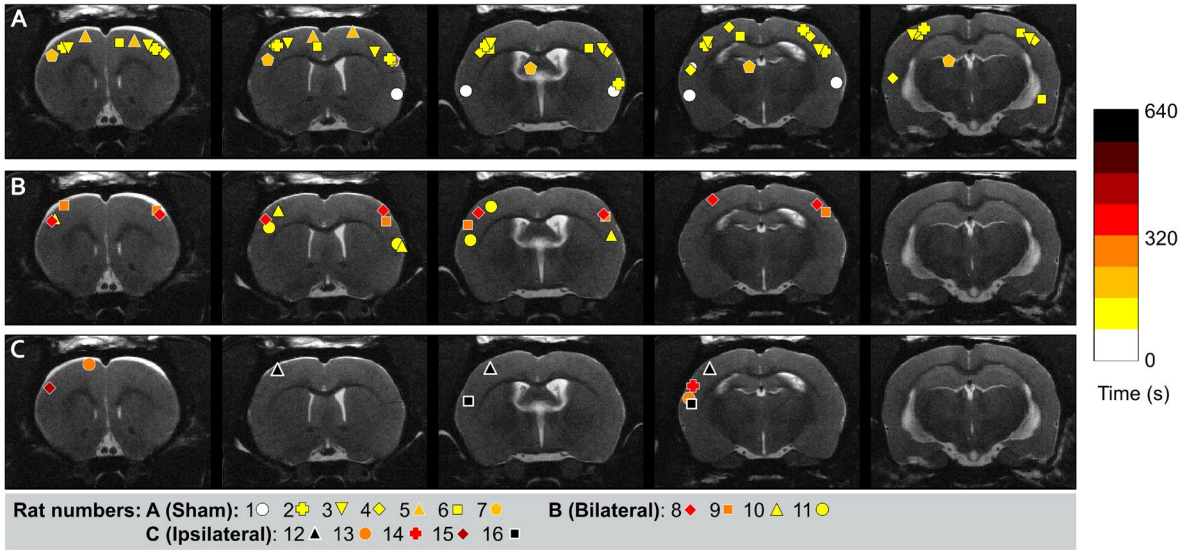

Figure 2. Location of the onset of pentylenetetrazol (PTZ) activation overlaid on the anatomic reference brain. The center of the seizure onset volume was calculated as a weighted average from the thresholded T-map for firstly activated regions. Each animal is shown with a colored symbol where the coloring represents the onset time in seconds (please see the color bar) when the location was activated relative to PTZ administration. **(A)** All 7 sham-operated experimental controls showed bilateral blood oxygenation level-dependent (BOLD) activation after PTZ administration. **(B)** Of the 9 TBI animals, 5 showed symmetric bilateral BOLD activation after PTZ administration. **(C)** In 4 of 9 TBI animals, the onset of PTZ-induced BOLD activation was ipsilateral (typically in the perilesional cortex), and gradually spread to the contralateral hemisphere.

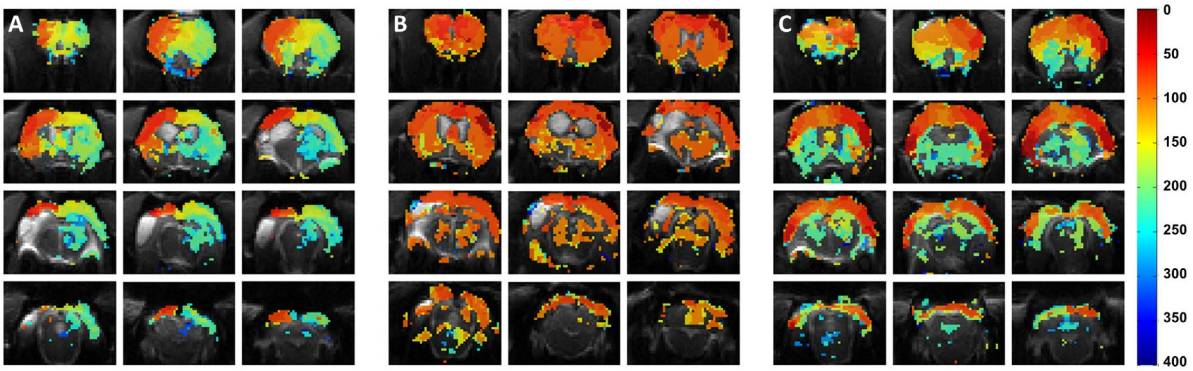

Figure 3. Map of BOLD onset times induced by pentylenetetrazol (PTZ) at voxel level. PTZ first activated the cortical areas, and later, the activation extended to the subcortical areas (e.g., striatum and thalamus). (A) A rat with TBI showing ipsilateral onset of the PTZ-induced cortical blood oxygenation level-dependent (BOLD) activation, which began rostral to the lesion, then spread to the contralateral cortex, and later to contralateral subcortical areas. (B) A rat with traumatic brain injury (TBI) showing bilateral activation. (C) A sham-operated experimental control showing bilateral activation. The color bar represents the time in seconds when voxels were activated relative to onset of the BOLD activation.

Delay to the onset of the BOLD response. In sham-operated experimental controls, the time delay between PTZ administration and the onset of the cortical BOLD response was comparable between hemispheres (left 132 ± 57 s vs. right 132 ± 57 s, n=6). Also, in TBI rats with bilateral onset of activation, the time from the PTZ injection to the onset of the cortical BOLD activation was comparable ipsilaterally (176 ± 54 s) and contralaterally (178 ± 52 s, n=4). In rats with ipsilateral onset of cortical activation, the time to onset of the cortical BOLD activation was faster in the perilesional cortex than in the contralateral cortex (406 ± 178 s *vs.* 508 ± 140 s, $p < 0.05$). Interestingly, the delay from the PTZ injection to the onset of the BOLD activation was longer in TBI rats with an ipsilateral onset (406 ± 178 s) than in TBI rats with a bilateral onset (176 ± 54 s), or in sham-operated experimental controls (132 ± 58 s; all $p< 0.05$).

Duration of the cortical BOLD response. Duration of the ipsilateral (relative to craniotomy) cortical BOLD response did not differ between the sham-operated controls (614 ± 196 s), TBI rats with a bilateral cortical onset (559 ± 132 s), or TBI rats with an ipsilateral cortical onset (497 ± 133 s). The duration of the contralateral cortical BOLD response also did not differ between groups (data not shown).

PTZ-induced thalamic BOLD response. The delay to activation of the ipsilateral (left) thalamus was 268 ± 93 s in sham-operated controls (6/6 rats had ipsilateral thalamic activation), 237 ± 71 s in rats with a bilateral BOLD onset (4/4 rats), and 516 ± 136 s in rats with an ipsilateral bold onset (2/5 rats).

Correlation of LFP activation and the BOLD response. The latency to the seizure onset in the contralateral cortical LFP electrode strongly correlated with the latency to the contralateral cortical BOLD onset (n=14, r=0.960, p<0.001).

Post-TBI brain pathology

Photomicrographs of representative cases summarizing the cortical and thalamic pathologies are shown in **Figs. 4 and Supplementary Fig. 1**. The area of cortical lesion in rats with ipsilateral (25.6 ± 13.3 mm^2) or bilateral BOLD onset (34.9 ± 5.8 mm^2) did not differ (p>0.05). Also, there was no correlation between the cortical lesion area and delay to BOLD activation or duration of ipsilateral or contralateral BOLD response (all p>0.05).

Analysis of GFAP-stained preparations revealed that 4 of the 5 rats with an ipsilateral onset of the BOLD response showed widespread perilesional inflammation, particularly rostrally, at 2 months post-TBI **(Fig. 4G),** whereas only 1 of the 4 animals with a bilateral onset had comparable GFAP staining. When quantifying the perilesional astrocytosis along the rostrocaudal edge of the lesion core, we detected a trend toward more intense GFAP-immunopositivity in rats with an ipsilateral rather than a bilateral onset of the BOLD response, particularly rostrally (glial score 217 ± 69 *vs.* 176 ± 32, respectively, p=0.33)(**Fig. 4G**).

All injured animals showed calcifications in the ipsilateral thalamus **(Figs 4D, Supplementary Fig. 2)**. Interestingly, rats with an ipsilateral PTZ-induced BOLD response had a trend towards lower mean calcification score (1.3 ± 1.0) than rats with a bilateral BOLD response (2.8 ± 0.5; p=0.06)(**Supplementary Fig. 2D**). Perilesional iron deposits were common in both subgroups **(Fig. 4B)**.

The density of the myelin fibers in the ipsilateral S1 cortex (layers V-VI) relative to contralateral side did not differ between rats with an ipsilateral (79% of that contralaterally) or bilateral (67%) onset of the BOLD response (p>0.05).

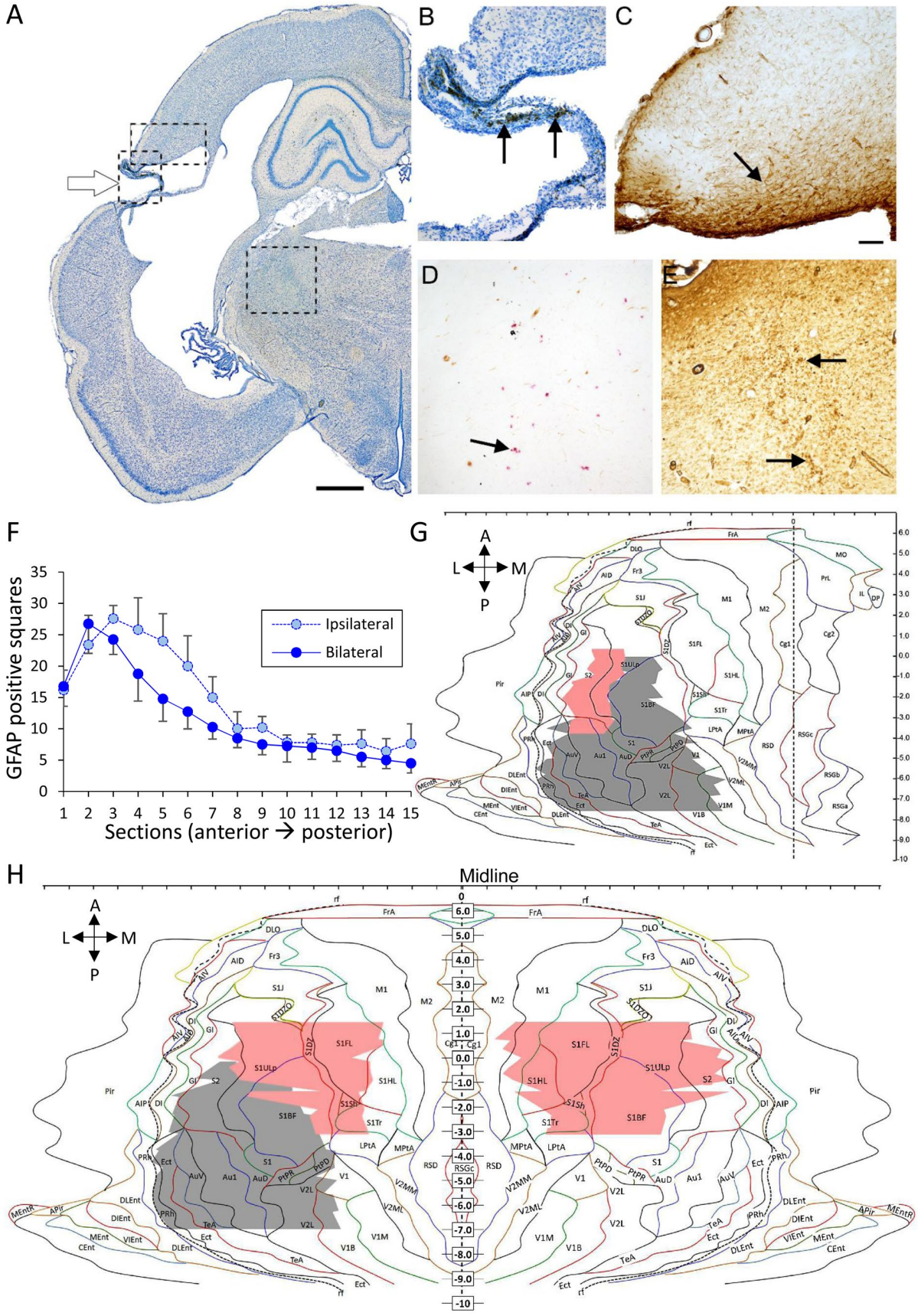

Figure 4. Photomicrographs of histologic sections from a rat with TBI and ipsilateral onset of pentylenetetrazol (PTZ)-induced BOLD activation. (A) A coronal thionin-stained section from the lesion core (open arrow). Dashed boxes are presented in higher magnification in

panels B-E. **(B)** The perilesional cortex showed intense iron staining (arrows). **(C)** A wide (100-400 µm) perilesional band of GFAP-positive astrogliosis (arrow). **(D)** Alizarin staining showed very small scattered calcium deposits in the ipsilateral thalamus (arrow). **(E)** Ox-42 immunostaining indicated microglial clusters in the ipsilateral thalamus. **(F)** A line graph showing the mean number of GFAP-positive 100x100 µm squares (y-axis) at 15 rostrocaudal levels (x-axis) in rats with ipsilateral or bilateral BOLD onset. Note a trend towards increased gliosis in the ipsilateral BOLD onset group (sections 3-8, p=0.226). Unfolded cortical maps showing the location of TBI-induced lesion (grey) and BOLD onset area (red) on cortical surface in **(G)** a rat with ipsilateral BOLD onset and **(H)** bilateral BOLD onset. Letters refer to the different cytoarchitectonic regions, according to rat brain atlas of Paxinos and Watson[58]. Abbreviations: A, anterior, GFAP, glial fibrillary acidic protein; L, lateral; M, medial; P, posterior. Data in panel F is shown as mean ± standard error of the mean. Scale bars = 1 mm in panel A and 100 µm in panel B-E.

Discussion

The present study assessed the onset zone of PTZ-provoked fMRI BOLD activation at 2 months after lateral FPI-induced TBI to define the hyperexcitable area during the time period when some of the animals were expected to be undergoing epileptogenesis. Our data indicated that the perilesional cortex was hyperexcitable in a subpopulation of rats at 2 months post-TBI.

PTZ test for the diagnosis of epileptogenesis

Epileptogenesis refers to the development and extension of tissue capable of generating spontaneous seizures, resulting in the development of an epileptic condition and/or progression of established epilepsy[38]. Thus, an increase in seizure susceptibility precedes the appearance of spontaneous seizures, and should be detectable by methodologies used, for example, to determine the localization of the seizure onset in patients evaluated for epilepsy surgery.

Chemoconvulsant PTZ (Metrazol®) in combination with SPECT is used to image hyperperfusion areas concordant with the cortical seizure onset zone in drug-refractory patients evaluated for epilepsy surgery[39-41]. In Supplementary material, we present in more detail one of those cases with drug-refractory PTE after childhood TBI. Overall, Metrazol®-induced ictal hyperperfusion areas in SPECT showed 88% concordance with electroclinical

findings in patients with extratemporal lobe seizures, and 82% concordance in patients with temporal lobe seizures[41]. Other human studies demonstrate a positive 77% correlation between spontaneous and electrically-induced seizures, and a 60% correlation between spontaneous and bicuculline-induced seizures[42]. Therefore, we hypothesized that PTZ-fMRI would reveal hyperexcitable brain areas in animals undergoing epileptogenesis at 2 months post-TBI.

fMRI revealed the perilesional cortex as a hyperexcitable area in a subpopulation of rats with TBI

PTZ is commonly used to test for seizure-susceptibility in genetically modified mice, inbred mice and rats with spontaneous seizures, and animals exposed to various epileptogenic brain injuries, including TBI[28,43-46]. The combination of PTZ administration with fMRI is used to image spatio-temporal evolution of seizure-induced BOLD responses and their suppression by an antiepileptic drug, ethosuximide, in the brains of normal animals[47]. The present study is the first to apply PTZ-fMRI to localize the BOLD onset zone in animals undergoing epileptogenesis due to brain injury.

As the previous and present data show, lateral FPI induces cortical damage with an epicenter in the polymodal auditory cortex, extending laterally down to the perirhinal cortex and caudally to the postrhinal cortex[33]. Available video-EEG monitoring data suggest that approximately 15% of animals exhibit spontaneous seizures at 2 months, 25% to 30% at 6 months, and 50% at 12 months post-TBI, and the evolution of pathology and epileptogenesis is largely variable between animals[9-12,48]. Thus, we expected that some, but not all, animals in the cohort investigated at 2 months post-TBI would show cortical BOLD activation when exposed to systemic PTZ.

In approximately 50% of our rats with TBI, PTZ-evoked seizures induced a BOLD response in the perilesional cortex rostral and medial/lateral to the lesion cavity, suggesting ongoing excitability and development of a seizure focus adjacent to the cortical lesion core. In all TBI cases, the BOLD onset was in the rostral aspect of the lesion, independent of the exact lesion location on the cortical mantle. Our data using noninvasive fMRI corresponds with recent electrophysiology studies using chronic intracortical recordings, showing a perilesional cortical onset of spontaneous seizures after lateral FPI-induced TBI[11,15]. Importantly, Bragin and coworkers also demonstrated that rats destined to develop PTE

exhibited pathologic high-frequency oscillations as well as repetitive pathologic high-frequency oscillations and EEG spikes in the perilesional cortex even before the appearance of spontaneous seizures, i.e., during epileptogenesis[15]. In 50% of our TBI rats and in sham-operated experimental controls, the onset the BOLD response appeared bilaterally in the cortex, corresponding to the pattern of PTZ-induced BOLD activation in normal rats[22,24,49]. These observations suggest that the evolution of epileptogenesis within the study cohort was variable, as expected based on previous studies[9-12,28].

In addition to the pattern of activation, the latency from the PTZ injection to the onset of the BOLD response varied between the animal groups. In particular, the latency was longer in TBI rats with a unilateral onset of the BOLD response compared to TBI rats with a bilateral onset. Interestingly, there was no correlation between the lesion severity and hyperexcitablity assessed by correlating the cortical lesion area with the latency to PTZ-induced BOLD activation or its duration. Pharmacokinetic studies indicate that lipophilic PTZ rapidly penetrates the blood-brain-barrier after systemic administration, suggesting rapid bilateral engagement of GABA-A receptors[50,51]. Therefore, we consider it unlikely that the delayed onset of the unilateral BOLD response in a subgroup of TBI animals could be explained by a reduced ipsilateral cortical vascular density or blood-brain-barrier penetration. As the BOLD response in the seemingly normal contralateral cortex was also delayed, we do not consider that a misplaced PTZ injection into the intraperitoneal cavity could explain the group differences either, as 4 of the 5 animals with an ipsilateral BOLD response had a delayed response onset compared with other animals. A slower spread of seizure activity in the thalamo-cortical pathways and corpus callosum due to white matter damage could slow down the spread of PTZ-induced BOLD activation in the injured brain.

Therefore, we next we assessed the pathologic substrate for unilateral onset of BOLD activation. We did not observe any apparent differences in the lesion area or in the location or number of perilesional iron deposits between TBI rats with an ipsilateral or bilateral onset of the BOLD response (data not shown). The severity of myelin damage in layers V-VI in the perilesional cortex also did not differ between groups, which could have affected the thalamo-cortical spread of the seizure activity and consequent BOLD activation[34]. In contrast to our expectations, animals with an ipsilateral onset of the PTZ-induced BOLD response had almost no calcium deposits in the ipsilateral thalamus. Instead, rats with a bilateral BOLD onset had robust “mature” stone-like thalamic calcifications ipsilaterally, suggesting that

thalamic calcifications were not responsible for the asymmetry in the cortical BOLD responses in this subgroup of animals. Assessment of GFAP-positive astrocytosis indicated that 4 of the 5 animals with an ipsilateral BOLD response had perilesional astrocytosis, whereas only 1 of the 4 rats with a bilateral BOLD response had a similar degree of perilesional GFAP-immunopositivity. Moreover, the width of astrogliotic rim appeared wider, particularly rostrally, in rats with ipsilateral BOLD onset as compared to that in rats with bilateral BOLD onset. Even though further studies with larger animal cohorts are needed, our findings suggest that the prolonged presence of an inflammatory milieu could enhance the evolution of perilesional hyperexcitability, resulting in focal activation of the BOLD response in the perilesional cortex when rats were exposed to systemic PTZ.

Taken together, TBI animals with a faster bilateral onset of BOLD activation had large cortical lesions, white matter damage, and their areas of thalamic calcification were even larger than that in rats with an ipsilateral onset of the BOLD response. Therefore, further studies are required to elucidate the mechanisms of delayed asymmetric perilesional BOLD activation in a subpopulation of rats with TBI. Also, interrelationship between focal hyperexcitability and hyper-connectivity, which was recently described by Harris et al after unilateral controlled cortical impact in rats[52] warrants future studies. Interestingly, a delayed hippocampal BOLD response was observed in one rat only, opposing the idea of a primary epileptogenic focus in the hippocampus.

Methodologic issues

fMRI with submillimeter spatial resolution and full brain coverage provides a unique approach to localizing the hyperexcitable zone during epileptogenesis in rats. The temporal resolution of 4 s, which is approximately twice larger than often used in fMRI was used to guarantee long enough artefact free period of LFP recordings between volumes, and to improve the stability of data in long scans. This temporal resolution does not allow for detailed tracking of the seizure spread, but it was sufficient to localize the onset zone in the perilesional cortex and differentiate subgroups of animals with either bilateral or unilateral onset. Probably the most significant experimental compromise in animal fMRI experiments is the need for anesthesia to immobilize the animals and alleviate stress. In the present work, we sedated rats by medetomidine infusion. Although any anesthesia or sedation is likely to have some modulatory effect on brain activity and the BOLD fMRI response, we recently

demonstrated that the fMRI response to chemically-induced seizures under medetomidine sedation is similar to that in an awake state[53].

Previous fluoro-deoxyglucose and c-Fos activation studies in normal uninjured rats[23,54-56] showed that systemic administration of PTZ triggered bilateral activation of the pathway from the hypothalamic mammillary nucleus to the anterior thalamic nucleus that spread to the somatosensory cortex. We were unable to detect a mamillo-thalamic spread of the BOLD response in sham-operated or injured animals, which may be due to the 4-s temporal resolution of our fMRI signal.

We have previously shown that cerebral blood flow (CBF) as measured by arterial spin labeling (ASL) is consistently reduced in chronic phase 8-9 months after TBI in in perilesional cortex[57] which may potentially influence the amplitude of BOLD response. However, we have previously shown that neurovascular coupling is preserved in ipsilateral cortex outside the primary lesion[34], so we are confident that fMRI is able to detect robust activation caused by PTZ.

Conclusions

Our findings demonstrated that the PTZ-induced BOLD response begins in the perilesional cortex in a subpopulation of rats at 2 months post-TBI, suggesting the ongoing evolution of an epileptogenic cortical focus. Similarly, PTZ-SPECT in a patient with PTE indicated perilesional hyperexcitability. Further analyses using PTZ-fMRI or PTZ-SPECT to reveal the evolution and localization of the epileptogenic zone after experimental TBI are warranted. Moreover, the contribution of chronic perilesional cortical inflammation, evolution of thalamic pathology to post-traumatic epileptogenesis requires further exploration.

Acknowledgements

We thank Merja Lukkari, Maarit Pulkkinen, and Jarmo Hartikainen for their excellent technical help and Raimo Salo for statistical advice. This study was supported by the Academy of Finland (AP, OG, XENE, ASL) and the FP7-HEALTH project 602102 (EPITARGET; AP, OG).

References

1. Herman, S.T. (2002). Epilepsy after brain insult: targeting epileptogenesis. Neurology 59, S21–S26.
2. Hesdorffer, D.C., Logroscino, G., Cascino, G., Annegers, J.F., and Hauser, W.A. (1998). Risk of unprovoked seizure after acute symptomatic seizure: effect of status epilepticus. Ann. Neurol. 44, 908–912.
3. Annegers, J.F., Hauser, W.A., Coan, S.P., and Rocca, W.A. (1998). A population-based study of seizures after traumatic brain injuries. N. Engl. J. Med. 338, 20–4.
4. Pitkänen, A., and Immonen, R. (2014). Epilepsy related to traumatic brain injury. Neurotherapeutics 11, 286–96.
5. Frey, L.C. (2003). Epidemiology of posttraumatic epilepsy: a critical review. Epilepsia 44 Suppl 1, 11–7.
6. Salazar, A.M., and Grafman, J. (2015). Post-traumatic epilepsy. clinical clues to pathogenesis and paths to prevention. Handb. Clin. Neurol. 128, 525–538.
7. Semah, F., Picot, M.C., Adam, C., Broglin, D., Arzimanoglou, A., Bazin, B., Cavalcanti, D., and Baulac, M. (1998). Is the underlying cause of epilepsy a major prognostic factor for recurrence? Neurology 51, 1256–1262.
8. Englander, J., Bushnik, T., Duong, T.T., Cifu, D.X., Zafonte, R., Wright, J., Hughes, R., and Bergman, W. (2003). Analyzing risk factors for late posttraumatic seizures: A prospective, multicenter investigation. Arch. Phys. Med. Rehabil. 84, 365–373.
9. Kharatishvili, I., Nissinen, J.P., McIntosh, T.K., and Pitkänen, A. (2006). A model of posttraumatic epilepsy induced by lateral fluid-percussion brain injury in rats. Neuroscience 140, 685–697.
10. Shultz, S.R., Cardamone, L., Liu, Y.R., Hogan, R.E., Maccotta, L., Wright, D.K., Zheng, P., Koe, A., Gregoire, M.-C., Williams, J.P., Hicks, R.J., Jones, N.C., Myers, D.E., O'Brien, T.J., and Bouilleret, V. (2013). Can structural or functional changes following traumatic brain injury in the rat predict epileptic outcome? Epilepsia 54, 1240–50.
11. Reid, A.Y., Bragin, A., Giza, C.C., Staba, R.J., and Engel, J. (2016). The progression of electrophysiologic abnormalities during epileptogenesis after experimental traumatic brain injury. Epilepsia 57, 1558–1567.
12. Wang, X., Wang, Y., Zhang, C., Liu, C., Zhao, B., Wei, N., Zhang, J.G., and Zhang, K. (2016). CB1 receptor antagonism prevents long-term hyperexcitability after head injury by regulation of dynorphin-KOR system and mGluR5 in rat hippocampus. Brain Res. 1646, 174–181.
13. Pitkänen, A., Immonen, R.J., Gröhn, O.H.J., and Kharatishvili, I. (2009). From traumatic brain injury to posttraumatic epilepsy: what animal models tell us about the process and treatment options. Epilepsia 50 Suppl 2, 21–9.
14. Curia, G., Levitt, M., Fender, J.S., Miller, J.W., Ojemann, J., and D'Ambrosio, R. (2011). Impact of injury location and severity on posttraumatic epilepsy in the rat: Role of frontal neocortex. Cereb. Cortex 21, 1574–1592.

15. Bragin, A., Li, L., Almajano, J., Alvarado-Rojas, C., Reid, A.Y., Staba, R.J., and Engel, J. (2016). Pathologic electrographic changes after experimental traumatic brain injury. Epilepsia 57, 735–45.
16. Thornton, R.C., Rodionov, R., Laufs, H., Vulliemoz, S., Vaudano, A., Carmichael, D., Cannadathu, S., Guye, M., McEvoy, A., Lhatoo, S., Bartolomei, F., Chauvel, P., Diehl, B., De Martino, F., Elwes, R.D.C., Walker, M.C., Duncan, J.S., and Lemieux, L. (2010). Imaging haemodynamic changes related to seizures: comparison of EEG-based general linear model, independent component analysis of fMRI and intracranial EEG. Neuroimage 53, 196–205.
17. Chaudhary, U.J., Centeno, M., Thornton, R.C., Rodionov, R., Vulliemoz, S., McEvoy, A.W., Diehl, B., Walker, M.C., Duncan, J.S., Carmichael, D.W., and Lemieux, L. (2016). Mapping human preictal and ictal haemodynamic networks using simultaneous intracranial EEG-fMRI. NeuroImage. Clin. 11, 486–93.
18. Chaudhary, U.J., Duncan, J.S., and Lemieux, L. (2013). Mapping hemodynamic correlates of seizures using fMRI: A review. Hum. Brain Mapp. 34, 447–66.
19. Tenney, J.R., Duong, T.Q., King, J.A., and Ferris, C.F. (2004). FMRI of brain activation in a genetic rat model of absence seizures. Epilepsia 45, 576–82.
20. Ingvar, M., Söderfeldt, B., Folbergrová, J., Kalimo, H., Olsson, Y., and Siesjö, B.K. (1984). Metabolic, circulatory, and structural alterations in the rat brain induced by sustained pentylenetetrazole seizures. Epilepsia 25, 191–204.
21. André, V., Pineau, N., Motte, J.E., Marescaux, C., and Nehlig, A. (1998). Mapping of neuronal networks underlying generalized seizures induced by increasing doses of pentylenetetrazol in the immature and adult rat: a c-Fos immunohistochemical study. Eur. J. Neurosci. 10, 2094–106.
22. Van Camp, N., D'Hooge, R., Verhoye, M., Peeters, R.R., De Deyn, P.P., and Van der Linden, A. (2003). Simultaneous electroencephalographic recording and functional magnetic resonance imaging during pentylenetetrazol-induced seizures in rat. Neuroimage 19, 627–36.
23. Eells, J.B., Clough, R.W., Browning, R.A., and Jobe, P.C. (2004). Comparative fos immunoreactivity in the brain after forebrain, brainstem, or combined seizures induced by electroshock, pentylenetetrazol, focally induced and audiogenic seizures in rats. Neuroscience 123, 279–92.
24. Keogh, B.P., Cordes, D., Stanberry, L., Figler, B.D., Robbins, C.A., Tempel, B.L., Green, C.G., Emmi, A., Maravilla, K.M., and Schwartzkroin, P.A. ([date unknown]). BOLD-fMRI of PTZ-induced seizures in rats. Epilepsy Res. 66, 75–90.
25. Kharatishvili, I., Nissinen, J.P., McIntosh, T.K., and Pitkänen, A. (2006). A model of posttraumatic epilepsy induced by lateral fluid-percussion brain injury in rats. Neuroscience 140, 685–97.
26. McIntosh, T.K., Vink, R., Noble, L., Yamakami, I., Fernyak, S., Soares, H., and Faden, A.L. (1989). Traumatic brain injury in the rat: Characterization of a lateral fluid-percussion model. Neuroscience 28, 233–244.

27. Huttunen, J.K., Gröhn, O., and Penttonen, M. (2008). Coupling between simultaneously recorded BOLD response and neuronal activity in the rat somatosensory cortex. Neuroimage 39, 775–85.
28. Kharatishvili, I., Immonen, R., Gröhn, O., and Pitkänen, A. (2007). Quantitative diffusion MRI of hippocampus as a surrogate marker for post-traumatic epileptogenesis. Brain 130, 3155–68.
29. Laitinen, T., Sierra, A., Pitkänen, A., Gröhn, O. (2010). Diffusion tensor MRI of axonal plasticity in the rat hippocampus. NeuroImage 51, 521-30.
30. Ndode-Ekane, X., Hayward, N., Gröhn, O., and Pitkänen, A. (2010). Vascular changes in epilepsy: Functional consequences and association with network plasticity in pilocarpine-induced experimental epilepsy. Neuroscience 166, 312-32.
31. Karhunen, H., Bezvenyuk, Z., Nissinen, J., Sivenius, J., Jolkkonen, J., Pitkänen, A. (2007). Epileptogenesis after cortical photothrombotic brain lesion in rats. Neuroscience 148, 314-24.
32. Mäkinen, S., van Groen, T., Clarke, J., Thornell, A., Corbett, D., Hiltunen, M., Soininen, H., and Jolkkonen, J. (2008). Coaccumulation of calcium and beta-amyloid in the thalamus after transient middle cerebral artery occlusion in rats. J Cereb Blood Flow Metab 28, 263–268.
33. Ekolle Ndode-Ekane, X., Kharatishvili, I., and Pitkänen, A. (2017). Unfolded Maps for Quantitative Analysis of Cortical Lesion Location and Extent after Traumatic Brain Injury. J. Neurotrauma 34, 459–474.
34. Niskanen, J.-P., Airaksinen, A.M., Sierra, A., Huttunen, J.K., Nissinen, J., Karjalainen, P.A., Pitkänen, A., and Gröhn, O.H. (2013). Monitoring functional impairment and recovery after traumatic brain injury in rats by FMRI. J. Neurotrauma 30, 546–56.
35. Lehto, L.J., Sierra, A., Corum, C.A., Zhang, J., Idiyatullin, D., Pitkänen, A., Garwood, M., and Gröhn, O. (2012). Detection of calcifications in vivo and ex vivo after brain injury in rat using SWIFT. Neuroimage 61, 761–72.
36. Silva, A., Koretsky, A., and Duyn, J. (2007). Functional MRI impulse response for BOLD and CBV contrast in rat somatosensory cortex. Magn Res Med 57, 1110-8.
37. Friston, K., Ashburner, J., Kiebel, S., Nichols, T., and Penny, W., eds. (2007). Statistical Parametric Mapping: The Analysis of Functional Brain Images. London: Academic Press.
38. Pitkanen, A., and Engel, J.J. (2014). Past and present definitions of epileptogenesis and its biomarkers. Neurotherapeutics 11, 231–241.
39. Barba, C., Di Giuda, D., Policicchio, D., Bruno, I., Papacci, F., and Colicchio, G. (2007). Correlation between provoked ictal SPECT and depth recordings in adult drug-resistant epilepsy patients. Epilepsia 48, 278–85.
40. Barba, C., Di Giuda, D., Fuggetta, F., and Colicchio, G. (2009). Provoked ictal SPECT in temporal and extratemporal drug-resistant epileptic patients: comparison of Statistical Parametric Mapping and qualitative analysis. Epilepsy Res. 84, 6–14.

41. Barba, C., Barbati, G., Di Giuda, D., Fuggetta, F., Papacci, F., Meglio, M., and Colicchio, G. (2012). Diagnostic yield and predictive value of provoked ictal SPECT in drug-resistant epilepsies. J. Neurol. 259, 1613–22.
42. Wieser, H.G., Bancaud, J., Talairach, J., Bonis, A., and Szikla, G. (1979). Comparative value of spontaneous and chemically and electrically induced seizures in establishing the lateralization of temporal lobe seizures. Epilepsia 20, 47–59.
43. Ates, N., Esen, N., and Ilbay, G. (1999). Absence epilepsy and regional blood-brain barrier permeability: the effects of pentylenetetrazole-induced convulsions. Pharmacol. Res. 39, 305–10.
44. Vezzani, A., Civenni, G., Rizzi, M., Monno, A., Messali, S., and Samanin, R. (1994). Enhanced neuropeptide Y release in the hippocampus is associated with chronic seizure susceptibility in kainic acid treated rats. Brain Res. 660, 138–43.
45. Blanco, M.M., dos Santos, J.G., Perez-Mendes, P., Kohek, S.R.B., Cavarsan, C.F., Hummel, M., Albuquerque, C., and Mello, L.E. (2009). Assessment of seizure susceptibility in pilocarpine epileptic and nonepileptic Wistar rats and of seizure reinduction with pentylenetetrazole and electroshock models. Epilepsia 50, 824–31.
46. Akhtari, M., Bragin, A., Moats, R., Frew, A., and Mandelkern, M. (2012). Imaging brain neuronal activity using functionalized magnetonanoparticles and MRI. Brain Topogr. 25, 374–88.
47. Brevard, M.E., Kulkarni, P., King, J.A., and Ferris, C.F. (2006). Imaging the neural substrates involved in the genesis of pentylenetetrazol-induced seizures. Epilepsia 47, 745–754.
48. Pitkänen, A., Bolkvadze, T., and Immonen, R. (2011). Anti-epileptogenesis in rodent post-traumatic epilepsy models. Neurosci. Lett. 497, 163–71.
49. DeSalvo, M.N., Schridde, U., Mishra, A.M., Motelow, J.E., Purcaro, M.J., Danielson, N., Bai, X., Hyder, F., and Blumenfeld, H. (2010). Focal BOLD fMRI changes in bicuculline-induced tonic-clonic seizures in the rat. Neuroimage 50, 902–9.
50. Vohland, H.W., and Zufelde, H. (1976). Factors responsible for reduced pharmacological activity in rats of pentetrazol administered orally. Naunyn. Schmiedebergs. Arch. Pharmacol. 293, 277–83.
51. Ramzan, I.M., and Levy, G. (1985). Kinetics of drug action in disease states. XIV. Effect of infusion rate on pentylenetetrazol concentrations in serum, brain and cerebrospinal fluid of rats at onset of convulsions. J. Pharmacol. Exp. Ther. 234, 624–8.
52. Harris, N., Verley, D., Gutman, B., Thompson, P., Yeh, H., and Brown, J. (2016). Disconnection and hyper-connectivity underlie reorganization after TBI: A rodent functional connectomic analysis. Exp Neurol 277, 124-138.
53. Airaksinen, A.M., Hekmatyar, S.K., Jerome, N., Niskanen, J.-P., Huttunen, J.K., Pitkänen, A., Kauppinen, R.A., and Gröhn, O.H. (2012). Simultaneous BOLD fMRI and local field potential measurements during kainic acid-induced seizures. Epilepsia 53, 1245–53.

54. Mirski, M.A., and Ferrendelli, J.A. (1986). Anterior thalamic mediation of generalized pentylenetetrazol seizures. Brain Res. 399, 212–23.
55. Mirski, M.A., and Ferrendelli, J.A. (1984). Interruption of the mammillothalamic tract prevents seizures in guinea pigs. Science 226, 72–4.
56. Mirski, M.A., and Ferrendelli, J.A. (1986). Selective metabolic activation of the mammillary bodies and their connections during ethosuximide-induced suppression of pentylenetetrazol seizures. Epilepsia 27, 194–203.
57. Hayward, N., Immonen, R., Tuunanen, P., Ndode-Ekane, X., Gröhn, O., Pitkänen, A. (2010). Association of chronic vascular changes with functional outcome after traumatic brain injury in rats. J Neurotrauma 27, 2203-19.
58. Paxinos, G. and Watson, C., 2010. The Rat Brain in Stereotaxic Coordinates. 6th ed., San Diego: Academic Press.

Supplementary figures and material

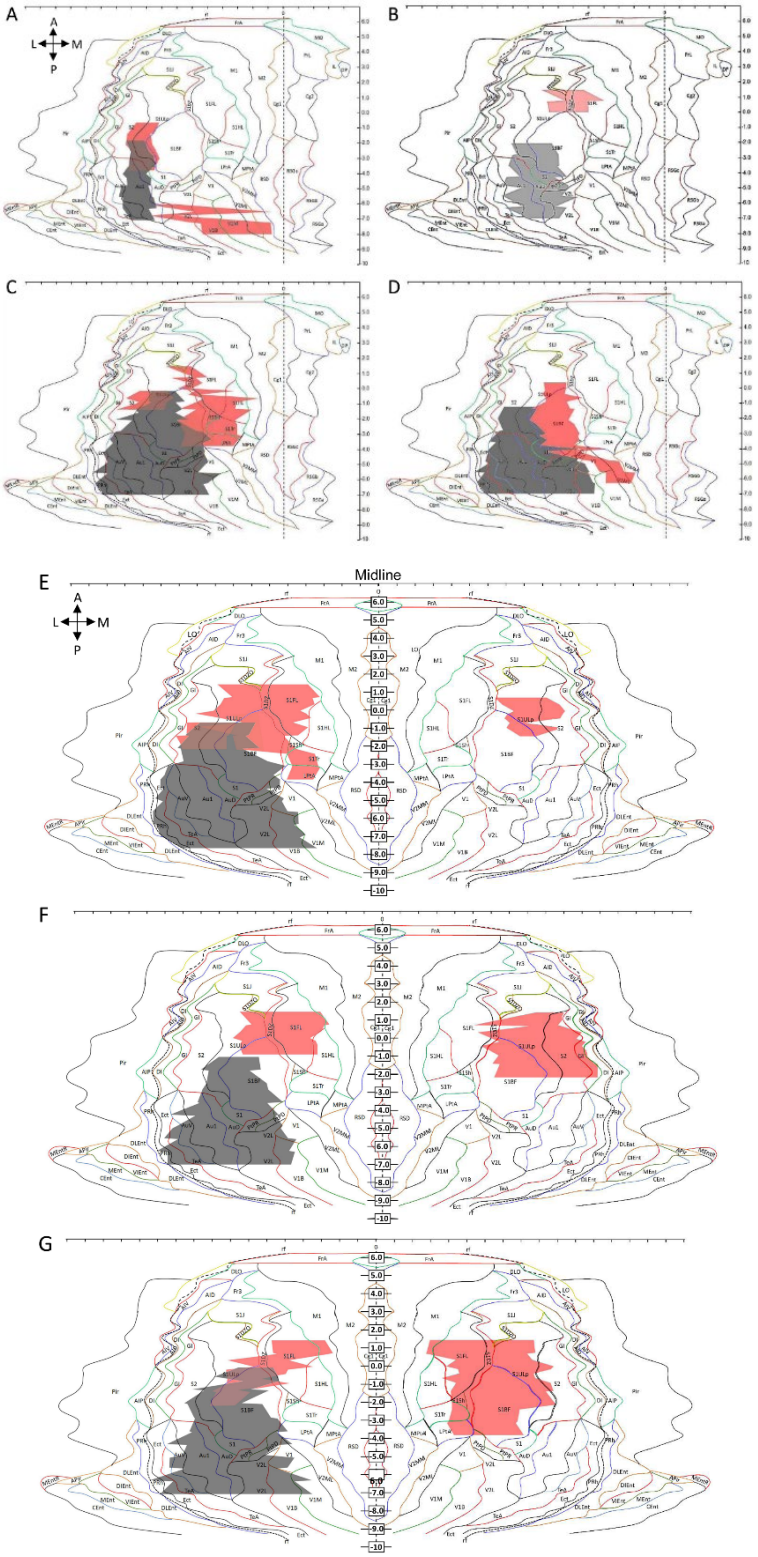

Supplementary Figure 1. Cortical unfolded maps showing the lesion location (grey) and BOLD onset region (red). **Panels A-D** are from rats with ipsilateral (left) and **panels E-G** from rats with bilateral BOLD onset.

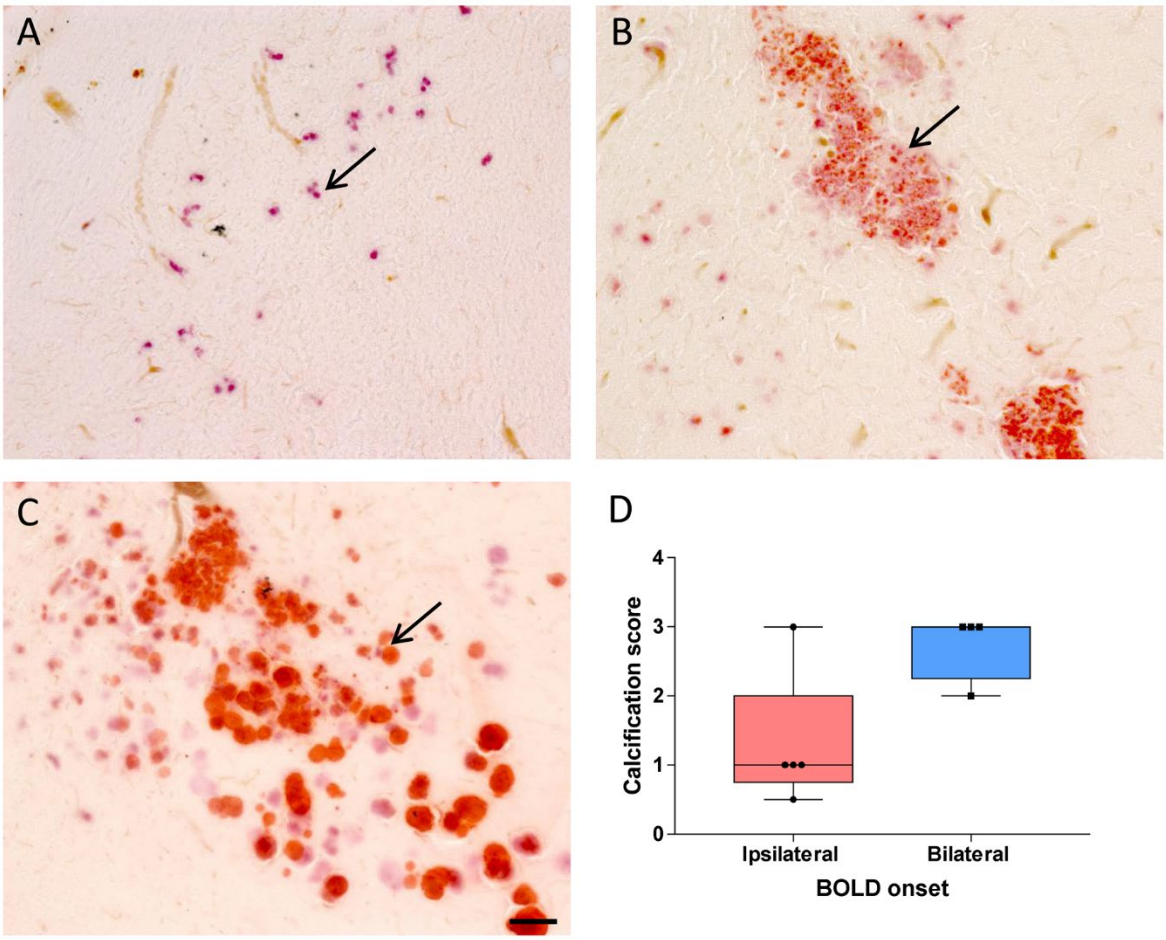

Supplementary Figure 2. Scoring of the severity of calcifications in the thalamus. **(A) Score 1,** scattered small calcifications (arrow). **(B) Score 2,** clusters of non-homogeneous calcifications (arrow) surrounded by scattered small calcifications. **(C) Score 3,** big stone-like solid round calcifications. **(D)** Box plot showing the calcification scores in the ipsilateral thalamus in rats with ipsilateral or bilateral PTZ-induced BOLD onset (p=0.06). Scale bar equals 50 µm (panels A-C).

PTZ-induced cortical activation in a patient with PTE – A case report

A 52-y old woman with a negative family history of epilepsy, normal pregnancy, delivery, and early psychomotor development suffered a TBI with a linear skull fracture of the left temporal and parietal bones due to a fall from a high chair at the age of 11 months. At 15 months of age, she exhibited focal motor status epilepticus (3 h) characterized by head and eye version toward the left, left hemiclonic manifestations, followed by left transient hemiparesis. Since the age of 6 y, she has exhibited seizures characterized by staring with arrest, guttural sounds, left dystonic posturing with non-patterned movements of the left arm, gestural and oroalimentary automatisms, and postictal amnesia. Sometimes her seizures were preceded by a right fronto-temporal migraine. Seizures occurred at a weekly frequency, especially during the menstrual cycle, usually in clusters. She also sporadically exhibited seizures characterized by unresponsiveness, head and eye version to the left, followed by stiffening of the left extremities. Repeated electroencephalograms showed diffuse epileptiform abnormalities with a right-sided prevalence. Brain MRI showed multiple small subcortical T2 and FLAIR hyperintensities with prevalence in the left hemisphere, and right thalamic porencephaly. Neuropsychologic assessment revealed diffuse cognitive impairment specifically involving praxis, memory, and logical reasoning.

After unsuccessful treatment with several antiepileptic drugs by the age of 44 y, she underwent presurgical evaluation at the Neurosurgery Department of Catholic University (Rome, Italy). A 1.5 T brain MRI showed multiple small subcortical bilateral T2 hyperintensities with a left-sided prevalence, T2 hyperintensity in the right hippocampus, and porencephaly in the right thalamus (Supplementary Fig. 3 panels C-D). Repeated video-electroencephalography (EEG) recordings captured seizures originating in the right parieto-occipital area (Supplementary Fig. 3 panel A). Interictal single photon emission tomography (SPECT) demonstrated right parieto-occipital hypoperfusion (Supplementary Fig. 3 panel E). Ictal SPECT during a seizure provoked by PTZ showed hyperperfusion in the right parieto-occipital area (Supplementary Fig. 3 panel F). For a complete description of the PTZ-provoked ictal SPECT protocol, see[41]. The patient was rejected from epilepsy surgery due to functional constraints, and submitted to vagal nerve stimulation with a subsequent reduction in seizure frequency.

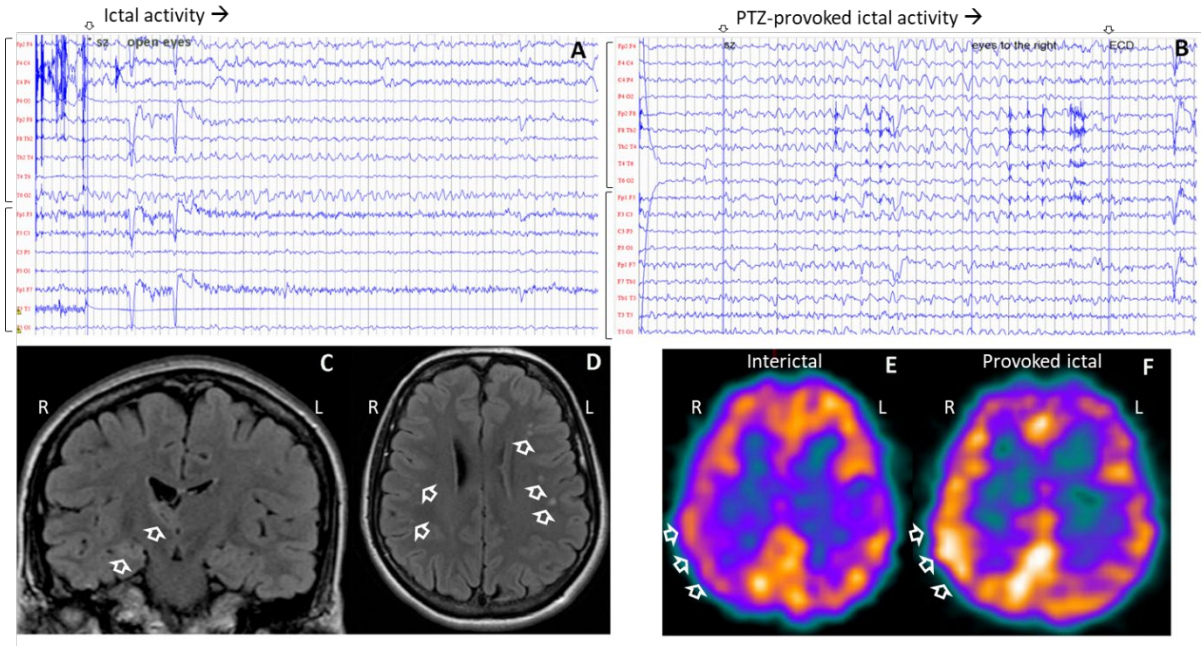

Supplementary Figure 3. 52-y female with post-traumatic epilepsy. (A) Electroencephalogram (EEG) recorded during a spontaneous ictal activity showing rhythmic theta activity that was most prominent in the right temporo-occipital area. Arrow indicates the beginning of the ictal activity. **(B)** EEG recorded during a pentylenetetrazol (PTZ)-provoked seizure, showing a diffuse discharge (between open arrows) with right temporo-occipital prevalence. The discharge was associated with eye version toward the right. **(C)** A coronal FLAIR brain MRI showing hyperintensity in the right hippocampus and right thalamic proencephalic area (see open arrows). **(D)** A FLAIR axial brain magnetic resonance imaging sequence showing multiple bilateral hemispheric hyperintensities, with left-sided prevalence (open arrows), possibly indicating diffuse axonal injury. **(E)** An interictal and **(F)** PTZ-provoked ictal single-photon emission computed tomography indicating a hypoperfusion (panel E, open arrows) and hyperperfusion (panel F, open arrows) pattern in the right posterior cortical region.

The procedure is part of the routine presurgical evaluation protocol performed at the Epilepsy Surgery Center of the Catholic University in Rome, and has been approved by the ethical standards committee on human experimentation of the Catholic University in Rome, Italy. The procedure is well tolerated and no major adverse effects have been observed. In the patient cohorts examined over the time, two patients have presented a transient mild rash that disappeared as soon as the pentyletetrazol administration was stopped. Due to the video surveillance and the presence of trained technicians, none of the patients has had any injuries

during the seizures following the PTZ injection, even in a case of secondary generalization[41]. Finally, all clinical data were pseudononymized.